Matching Coefficients for the Strong Coupling in the Standard Model and MSSM

[TTP06-20]

Matthias Steinhauser[a]

[a]Institut für Theoretische Teilchenphysik, Universität Karlsruhe, 76128 Karlsruhe, Germany

In this contribution we review the status of the decoupling coefficients for α_s both in the Standard Model (SM) and its minimal supersymmetric extension, the so-called MSSM. We stress the importance of a consistent treatment, in particular within the framework of the MSSM.

1. Motivation

The strong coupling constant, α_s, constitutes a fundamental parameter in the Standard Model (SM) and thus its precise numerical value is very important for many physical predictions. An interesting property of α_s is its scale dependence, in particular its strong rise for low and its small value for high energies which make perturbative calculations within the framework of QCD possible. The scale dependence is governed by the β function. However, in order to relate α_s at two different scales it is also necessary to incorporate threshold effects of heavy quarks which is achieved with the help of the so-called matching or decoupling relations. Thus, when specifying α_s it is necessary to indicate next to the scale also the number of active flavours.

A consistent treatment of the running and decoupling procedure requires the use of $(N-1)$-loop decoupling formulae together with N-loop expressions for the β function. As far as QCD is concerned, recently the four-loop matching relations have been computed by two independent groups [1,2]. Formally this would require the knowledge of the five-loop β function, however, currently only the four-loop terms are known [3,4].

The situation is different in the context of supersymmetry. In the limit where the number of active fermions and sfermions is equal the β function up to three loops is available since already quite some time [5], however, until recently only the one-loop matching conditions have been available in the literature. This gap has been closed in Ref. [6] where two-loop decoupling relations in the framework of the MSSM have been studied.

In this contribution we provide a brief overview on the current status, both for QCD, which is treated in Section 2, and SUSY-QCD, which can be found in Section 3.

2. Decoupling in QCD

A typical problem where the question of decoupling plays a crucial role occurs when two values of α_s, defined for different number of active flavours, shall be related to each other. E.g., consider the case where $\alpha_s^{(5)}(M_Z)$ shall be computed from the knowledge of $\alpha_s^{(4)}(M_\tau)$. In this example the decoupling constant has to provide a relation between $\alpha_s^{(4)}(\mu_b)$ and $\alpha_s^{(5)}(\mu_b)$ where μ_b is the matching scale where the bottom quark is decoupled.

In a more general way we define the decoupling constant via

$$g_s^{0\prime} = \zeta_g^0 g_s^0 \,, \tag{1}$$

where $g_s^0 = \sqrt{4\pi\alpha_s^0}$ is the bare strong coupling. In close analogy to the renormalization procedure it is possible to relate ζ_g^0 to the decoupling constants of the ghost-gluon vertex, the gluon propagator and the ghost propagator:

$$\zeta_g^0 = \frac{\tilde\zeta_1^0}{\tilde\zeta_3^0\sqrt{\zeta_3^0}} \,. \tag{2}$$

It is convenient to define the ζ's in a first step for bare quantities since then one-to-one relations between the N-loop contributions to the decoupling constants and the N-loop vacuum integrals can be established [7]. Sample diagrams up to four-loop order can be found in Fig. 1(a), (b) and (c). The technology up to three-loop order is well documented in the literature and publicly available programs exist (see, e.g., Refs. [8,9]). The development of the four-loop technology is quite new. The results of Ref. [1] are based on a program [10] where the so-called Laporta algorithm has been implemented in FORM [11].

Once the bare four-loop result for the decoupling relation is available it is straightforward to obtain the renormalized expression with the help of the usual renormalization constants (see, e.g., Ref. [12])

$$\zeta_g = \frac{Z_g}{Z_g'}\zeta_g^0 . \tag{3}$$

The analytical result for ζ_g can be found in Ref. [1] where only one constant, which was denoted by X_0, has not been known in analytical form but with high numerical precision. Meanwhile also this constant is available analytically [13] with the result

$$\begin{aligned} X_0 &= -384 a_5 + \frac{873}{2}\zeta_5 - \frac{53}{15}\pi^4 \ln 2 \\ &\quad - \frac{16}{3}\pi^2 \ln^2 2 + \frac{16}{5}\ln^5 2 \\ &\approx 1.8088795462083347414\ldots , \end{aligned} \tag{4}$$

where $a_5 = \mathrm{Li}_5(1/2)$ and $\zeta_5 \approx 1.036927755\ldots$.

In order to study the numerical impact of our result we consider the evaluation of $\alpha_s^{(5)}(M_Z)$

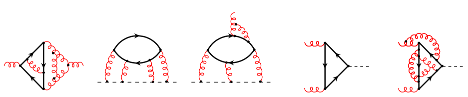

(a) (b) (c) (d) (e)

Figure 1. Sample diagrams for the gluon (a) and ghost (b) propagator and the ghost-gluon vertex (c). In (d) the lowest-order diagram is shown mediating the Higgs-gluon coupling in the SM and (e) shows an example for a five-loop diagram contributing to the coefficient function C_1.

from $\alpha_s^{(4)}(M_\tau)$, i.e. we apply our formalism to the crossing of the bottom quark threshold. In general one assumes that the value of the scale μ_b, where the matching has to be performed, is of order m_b. However, it is not determined by theory. Thus this uncertainty contributes significantly to the error of physical predictions. On general grounds one expects that while including higher order perturbative corrections the relation between $\alpha_s^{(4)}(M_\tau)$ and $\alpha_s^{(5)}(M_Z)$ becomes insensitive to the choice of the matching scale which we want to demonstrate in the following up to the five-loop order.

Starting from $\alpha_s^{(4)}(M_\tau) = 0.36$ we compute in a first step $\alpha_s^{(4)}(\mu_b)$ using N-loop accuracy. Afterwards $\alpha_s^{(5)}(\mu_b)$ is obtained where for consistency the $(N-1)$-loop matching equations have to be used. Finally, we compute $\alpha_s^{(5)}(M_Z)$ using again the N-loop in the β function.

In Fig. 2 the result for $\alpha_s^{(5)}(M_Z)$ as a functions μ_b is displayed for the one- to five-loop analysis. For illustration, μ_b is varied rather extremely, by almost two orders of magnitude. While the leading-order result exhibits a strong logarithmic behaviour, the analysis is gradually getting more stable as we go to higher orders. The five-loop curve is almost flat for $\mu_b \geq 1$ GeV and demonstrates an even more stable behaviour than the four-loop analysis of Ref. [7]. It should be noted that around $\mu_b \approx 1$ GeV both the three-, four- and five-loop curves show a strong variation which can be interpreted as a sign for the breakdown of perturbation theory. Note that for this analysis the unknown five-loop coefficient of the β function is set to zero.

An interesting connection between the decoupling constant discussed so far, which constitutes a fundamental quantity of QCD, and a building block for the production and decay of a SM Higgs boson is established by the all-order low-energy theorem [7] given by

$$C_1 = -\frac{1}{2}\frac{m_t^2 \partial}{\partial m_t^2} \ln \zeta_g^2 . \tag{5}$$

Eq. (5) relates ζ_g to the coefficient function appearing in the effective Lagrangian of an intermediate-mass Higgs boson to two, three and

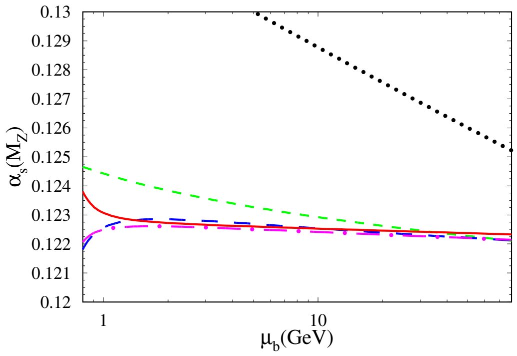

Figure 2. μ_b dependence of $\alpha_s^{(5)}(M_Z)$ calculated from $\alpha_s^{(4)}(M_\tau) = 0.36$ and $m_b = 4.7$ GeV. The procedure is described in the text. The dotted, short-dashed, long-dashed and dash-dotted line corresponds to one- to four-loop running. The solid curve includes the effect of the new four-loop matching term.

four gluons. It is conveniently written in the form

$$\mathcal{L}_{\rm eff} = -\frac{H^0}{v^0} C_1 \mathcal{O}_1 \,, \tag{6}$$

where the effective operator $\mathcal{O}_1$ is given by

$$\mathcal{O}_1 = \left(G^a_{\mu\nu}\right)^2 \,, \tag{7}$$

The appealing feature of Eq. (5) is the derivative with respect to m_t^2 since the $(N+1)$-loop dependence of ζ_g can be reconstructed from the knowledge of ζ_g to N-loop order. This is possible since m_t only enters in the combination $\ln \mu^2/m_t^2$. The five-loop result for C_1, which contains diagrams like the one in Fig. 1(e), can be found in Ref. [1]. It only contains the fermionic part of the five-loop β function as unknown coefficient.

3. Decoupling in the MSSM

In extensions of the SM similar considerations hold as for QCD. E.g., a typical problem in the minimal extension of the SM is the relation of the strong coupling at the GUT scale and the electroweak scale. In contrast to QCD many mass scales enter the decoupling procedure and thus beyond one-loop order both the calculation and the formulae become significantly more complicated although the very formalism drafted in the beginning of the previous Section remains the same. A further difference to QCD occurs in connection to the regularization scheme: since dimensional regularization breaks supersymmetry in this Section dimensional reduction is used (see Ref. [6] for more details).

At one-loop order only one mass scale enters at a time in the Feynman diagram and thus the exact formula is available. It is given by

$$(\zeta_g^{\rm SUSY})^2 = 1 + \frac{\alpha_s^{\rm (SUSY)}}{\pi} \left[-\frac{1}{6} L_t - \frac{1}{12} \sum_{s=1}^{n_s} L_{\tilde{q}_s} - \frac{n_{\tilde{g}}}{2} L_{\tilde{g}} \right] + \mathcal{O}\left(\alpha_s^2\right) \,, \tag{8}$$

where $L_x = \ln(\mu^2/m_x^2)$. Already in this formula one can see that a single choice for μ does not avoid possible large logarithms.

Sample Feynman diagrams for the two-loop calculation can be found in Fig. 3. As can be seen, in general several mass scales appear which make the analysis more involved. In Ref. [6] several scenarios have been considered in order to demonstrate the numerical effects. In particular for the following cases the decoupling constant has been evaluated

(A) $m_{\tilde{u}}, \ldots, m_{\tilde{b}} \gg m_{\tilde{t}}, m_{\tilde{g}}, m_t \gg m_b$

(B) $m_{\tilde{u}}, \ldots, m_{\tilde{b}}, m_{\tilde{t}} \gg m_{\tilde{g}}, m_t \gg m_b$

(C) $m_{\tilde{u}}, \ldots, m_{\tilde{b}}, m_{\tilde{t}}, m_{\tilde{g}} \gg m_t \gg m_b$

(D) $m_{\tilde{u}}, \ldots, m_{\tilde{b}}, m_{\tilde{t}}, m_{\tilde{g}}, m_t \gg m_b \,,$

where $m_{\tilde{u}}, \ldots, m_{\tilde{t}}$ are the squark masses, $m_{\tilde{g}}$ is the gluino mass and m_t, m_b are the top and the bottom quark mass, respectively. Masses separated by a comma are assumed to have the same order of magnitude and for each "$\gg$" sign a decoupling constant and a corresponding matching scale have to be introduced. Note that case (B) corresponds to so-called split SUSY and in case (C) all supersymmetric masses are considered as heavy with respect to the SM ones.

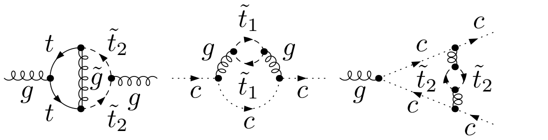

Figure 3. Sample diagrams contributing to the decoupling constants ζ_3^0, $\tilde{\zeta}_3^0$ and $\tilde{\zeta}_1^0$.

Squark masses are always taken to be larger than the top quark mass. Analytic results for the individual decoupling constants can be found in Ref. [6].

Let us in the following discuss the numerical effects for various examples.

In Fig. 4 which shows $\alpha_s(\mu_{\rm GUT})$ for scenario (C) as a function of the two matching scales $\mu_{\rm th,1}$ and $\mu_{\rm th,2}$, the dependence on the matching scales and the loop order is exemplified. Each matching scale is varied by a factor of ten around the default value 1000 GeV and 400 GeV, respectively.

One can clearly see how the result stabilizes as soon as two-loop running and one-loop matching

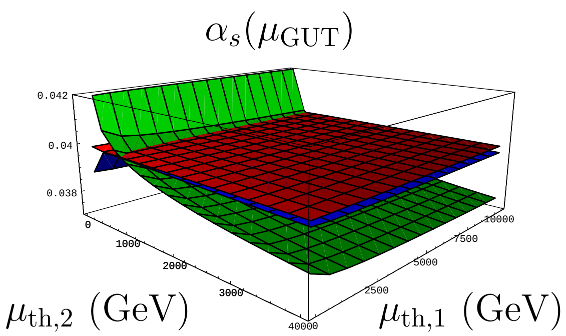

Figure 4. $\alpha_s(\mu_{\rm GUT})$ for $\mu_{\rm GUT} = 10^{16}$ GeV as a function of the two matching scales $\mu_{\rm th,1}$ and $\mu_{\rm th,2}$. The lower (green), middle (blue) and upper (red) planes correspond to one-, two- and three-loop running accompanied with the corresponding order in the decoupling relation for the scenario (C).

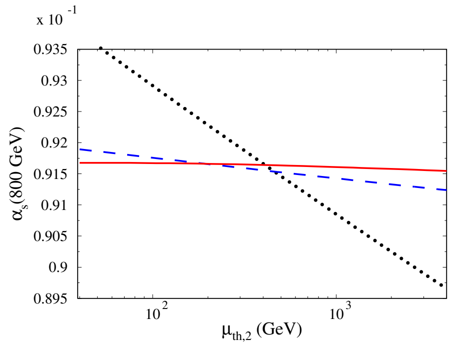

Figure 5. $\alpha_s(800\text{ GeV})$ as a function of $\mu_{\rm th,1}$ for scenario (C). The dotted, dashed and full lines correspond to one-, two- and three-loop running.

(middle plane) is included. The three-loop corrections stabilize the dependence of α_s on $\mu_{\rm th,1}$ and $\mu_{\rm th,2}$ even more (upper plane), such that the result is practically independent of the matching scales within a wide range around their default values. Within the considered range of $\mu_{\rm th,1}$ and $\mu_{\rm th,2}$, the variation of $\alpha_s(\mu_{\rm GUT})$ is 13.8/1.6/0.3% at 1-/2-/3-loop order.

Another practical application of our results is shown in Fig. 5[1], where the strong coupling is computed for $\sqrt{s} = 800$ GeV which is the proposed center-of-mass energy of a future International Linear Collider (ILC) is computed. While for $\mu_{\rm th,2} \approx 200$ GeV the two- and three-loop result practically give the same value for α_s, for $\mu_{\rm th,2} = 2000$ GeV the shift induced by the new three-loop terms is comparable with the uncertainty induced by the experimental value for $\alpha_s(M_Z)$. The latter is given by ± 0.0012 assuming an error of ± 0.002 for $\sqrt{s} = M_Z$. This underlines once more the importance of the two-loop decoupling and three-loop running terms.

In Fig. 6 we combine our findings for the evolution of the inverse strong coupling at the GUT scale (yellow band) with the two-loop order results for the strong (α_s, red band), the electromagnetic (α_1, blue band) and the weak coupling (α_2, green band) (for a precise definition, see Ref. [14], and references therein). The wide er-

[1]Note that the plot in Ref. [6] corresponds to $\alpha_s(M_Z) = 0.118$ and not to $\alpha_s(M_Z) = 0.120$ which was used for the strong coupling in the $\overline{\rm DR}$ scheme.

ror bands correspond to the present experimental accuracy for the gauge couplings and the supersymmetric mass spectrum of the SPS1a reference point. The inner bands account for the expected improvements in the absolute errors due to the future experimental analysis at LHC+LC.

Depending on the scenario, i.e. the particle masses in the MSSM respectively their hierarchy, a significant numerical effect can be observed. Whereas for scenario B (upper plot) the shift due to the three-loop is relatively small the yellow band for scenario C (lower plot) is outside the LHC error band. This demonstrates that it is important to include two-loop corrections in the analyses considering the unification of couplings but also the evaluation of low-energy parameters from unified parameters at high energies.

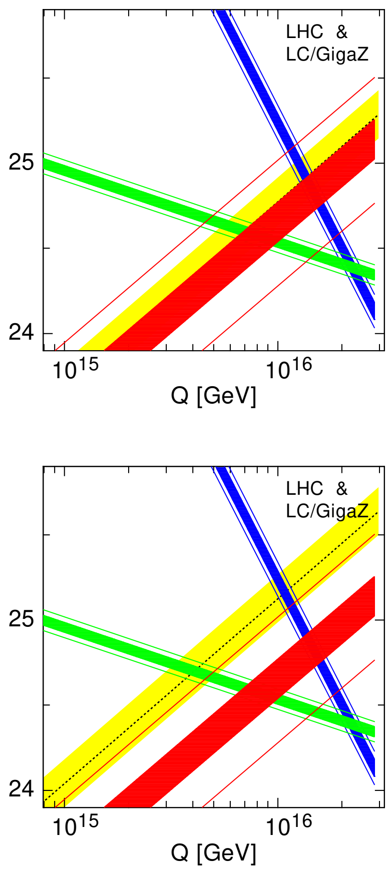

Figure 6. Running of the inverse couplings $1/\alpha_i$, $i = 1$ (see main text for details).

Acknowledgements

I would like to thank R. Harlander, L. Mihaila and Y. Schröder for the pleasant collaboration leading to the results presented in this contribution. I would like to thank the organizers of Loops and Legs 2006 for the pleasant atmosphere during the conference. This work was supported by the DFG through SFB/TR 9.

REFERENCES

1. Y. Schröder and M. Steinhauser, JHEP **0601** (2006) 051 [arXiv:hep-ph/0512058].
2. K. G. Chetyrkin, J. H. Kuhn and C. Sturm, Nucl. Phys. B **744** (2006) 121 [arXiv:hep-ph/0512060].
3. T. van Ritbergen, J. A. M. Vermaseren and S. A. Larin, Phys. Lett. B **400** (1997) 379 [hep-ph/9701390].
4. M. Czakon, Nucl. Phys. B **710** (2005) 485 [hep-ph/0411261].
5. I. Jack, D. R. T. Jones and C. G. North, Phys. Lett. B **386** (1996) 138 [arXiv:hep-ph/9606323].
6. R. Harlander, L. Mihaila and M. Steinhauser, Phys. Rev. D **72** (2005) 095009 [arXiv:hep-ph/0509048].
7. K. G. Chetyrkin, B. A. Kniehl and M. Steinhauser, Nucl. Phys. B **510** (1998) 61 [hep-ph/9708255].
8. M. Steinhauser, Phys. Rept. **364** (2002) 247 [hep-ph/0201075].
9. M. Steinhauser, Comput. Phys. Commun. **134** (2001) 335 [arXiv:hep-ph/0009029].
10. Y. Schröder, Nucl. Phys. Proc. Suppl. **116** (2003) 402 [hep-ph/0211288].
11. J. A. M. Vermaseren, arXiv:math-ph/0010025.
12. K. G. Chetyrkin, Nucl. Phys. B **710** (2005) 499 [hep-ph/0405193].
13. Y. Schröder, these proceedings.
14. B. C. Allanach, G. A. Blair, S. Kraml, H. U. Martyn, G. Polesello, W. Porod and P. M. Zerwas, arXiv:hep-ph/0403133.